"EXTREME PRECIPITATION EVENTS OVER NORTH-WESTERN EUROPE: GETTING WATER FROM THE TROPICS "

Enrico Scoccimarro[1,*], Silvio Gualdi[1], Simon O. Krichak[3],

[1] Fondazione Centro Euro-Mediterraneo sui Cambiamenti Climatici (CMCC), Bologna, Italy

[2] Istituto Nazionale di Geofisica e Vulcanologia (INGV), Bologna, Italy

[3] Department of Geosciences, Raymond and Beverly Sackler Faculty of Exact Sciences, Tel Aviv University, Tel Aviv, Israel

ABSTRACT

Our capability to adapt to extreme precipitation events is linked to our skill in predicting their magnitude and timing. Synoptic features (such as Atmospheric Rivers) developing over the North Atlantic Ocean are known as the source of the majority of water vapour transport into European mid-latitudes, and are associated with episodes of heavy and prolonged rainfall over UK and north western Europe. Thus, a better understanding of the North Atlantic atmospheric conditions prior the occurrence of extreme precipitation events over Europe could help in improving our capability to predict them. We build on atmospheric re-analyses at high spatial resolution, on a daily time scale, to highlight the anomalous path of the vertically integrated water content, transferring water from the western tropical North Atlantic to high latitudes and fuelling the storms developing in the North Atlantic sector, bound to affect Europe as responsible for the most intense precipitation events. The systematic link between anomalous north-eastward transport of vertically integrated water (precipitable water) from the western North Atlantic and anomalously high pressure patterns in the central North Atlantic, developing 5 days prior the extreme precipitation occurrence, suggest the central North Atlantic surface pressure as a potential precursor of extreme precipitation events.

1. INTRODUCTION

The identification of the origin of the water fuelling extreme precipitation episodes (EPEs) over Europe is a challenging issue with important implications for the predictions of high-impact events. The main role played by the North Atlantic ocean in providing water to EPEs over Europe has already been assessed in many studies [Gimeno et al., 2010a; Knippertz and Wernli, 2010; Winschall et al., 2012; Krichak et al., 2012; Krichak et al., 2015]. It is well known that moisture source regions affecting the European coasts are in a tropical-subtropical North-Atlantic corridor that extends from the Gulf of Mexico to the Europe [Gimeno et al., 2010b] and also that the main transport pathway away from the tropical Atlantic (the Atlantic region with the highest vertically integrated precipitable water content) is through the midlatitude storm tracks (mainly poleward of 30oN), indicating a direct transport of precipitable water (PW) from the tropics into high latitudes [Walker and Schneider, 2006; Pauluis et al., 2008]. Since the regions of intense poleward moisture fluxes, associated with EPEs over Europe are, in general, relatively narrow in longitude [Lavers et al., 2011, Lavers et al., 2013], this kind of fluxes have been named atmospheric rivers [ARs, Newel et al., 1992]. Recent works suggest that not only moisture export from the tropics can provide important vapour sources for ARs, but also midlatitude sources and convergences of vapour along their paths [Dacre et al., 2015] play a role. According to Dettinger et al. [2015] and Ramos et al. [2016] it seems that both
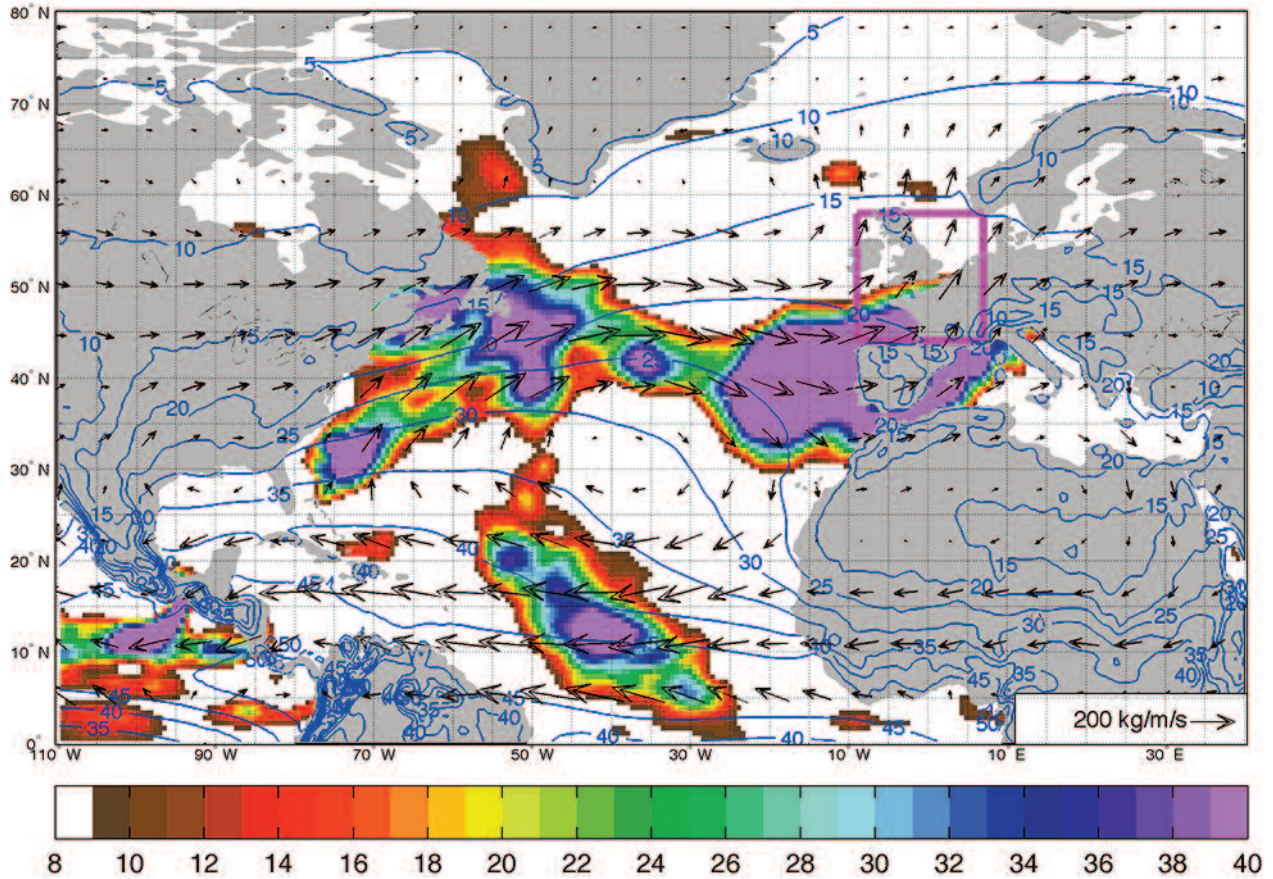
FIGURE 1. Composite of vertically integrated water transport IWT associated with extreme precipitation events over the investigated region (magenta box), averaged over the four days prior the extreme precipitation event and the day of occurrence. Colour patterns are IWT absolute value composite anomalies (IWTp99). Vectors are IWT composites, averaged over the same period, same as IWTp99, but these are not anomalies. Contour lines represent precipitable water (PW) climatology during September-November period. IWT Units are [$kgm^{-1}s^{-1}$]. PW Units are [Kgm^{-2}].

sources of water can be considered when investigating extreme precipitation events over Europe.

Most of the EPEs occurring over UK and north western Europe are associated with ARs: 8 of the 10 EPEs during the 1979-2011 period are related to ARs [Lavers and Villarini, 2013]. It has been demonstrated that ARs are responsible for more than 90% of the total poleward atmospheric water vapour transport through the middle latitudes [Newell and Zhu, 1992; Ralph and Dettinger, 2011]. In the following analysis the issue is additionally addressed by investigating the time evolution of water transport across the North Atlantic sector preceding extreme precipitation events over a specific sector of the north-western Europe [E1 region in Krichak et al., 2015, as highlighted by the magenta box in Figure 1]. The goal of the study is twofold: (i) to identify the atmospheric path of the water fuelling storms associated with EPEs over the E1 region and (ii) to investigate potential source of (short-term) predictability of such events, leveraging the characteristic foregoing large scale circulation pat-

terns appearing over the North Atlantic Ocean. The paper is organized as follows: Section 2 describes the re-analyses data set used, together with the methodology. Section 3 presents the results of the analyses, while section 4 discusses the main results and concludes the paper.

2. DATA AND METHODOLOGY

2.1 REFERENCE DATA

The Japanese 55-year re-analyses [JRA-55, Kobayashi et al., 2015] data set, having a spatial resolution of 0.5° longitude by 0.5° latitude and 60 vertical levels with top layer at 0.1 hPa is adopted. This data set has been demonstrated suitable for studies on vapour transport of remotely evaporated seawater [Kudo et al., 2014]. JRA-55 provides two dimensional fields such as precipitation (PREC), surface pressure (PRES), 10 meter winds (WIND) and evaporation (EVP), together with vertically integrated fields such as precipitable water

(PW) and integrated water transport (IWT) in its meridional (VWV) and zonal (UWV) components at 3 hourly time scale. The present study is based on daily values averaged from the available 3 hourly data. To reinforce our findings, we make use of multiple reanalysis [Nayak and Villarini, 2017]: the analysis described in the next subsection has been performed also using the National Aeronautics and Space Administration - NASA's Modern Era Retrospective-Analysis [MERRA; Rienecker et al., 2011]. MERRA has a spatial resolution of 0.5° latitude and 0.7o longitude, with 72 vertical levels, from the surface to 0.01 hPa. The present paper Figures 1 to 5 are based on JRA-55 reanalysis and confirmed by MERRA results in the corresponding Figures A1 to A5 shown in the supplemental material.

2.2 METHODOLOGY

The investigated period is 1979-2013 and only the autumn season (from September to November, SON) is considered. The choice of the season is determined by two factors: SON is the period of the year affected by the larger number of annual maxima of daily precipitation [Lavers et al., 2013] over the region of interest and during this season the contribution of North Atlantic moisture to precipitation events is more pronounced compared with the rest of the year [Winschall et al., 2014]. In the rest of the paper, we will refer to the period of analysis (3 months x 35 years) as PRESCLI. As a first step, we computed the time series (91 days x 35 years = 3185 values) of maximum precipitation, resulting from reanalysis data, over the British Isles-Europe's Atlantic coast (44N-58N, 9W-7E) region (Figure 1, magenta box - about 250 grid points). Within this time series we defined as extreme events the 32 cases exceeding the 99 percentile of the distribution resulting from the 3185 values (E1_EPEs). Extreme events counting refers to events lasting just 1 day. To define the large circulation anomalies associated with E1_EPEs we computed the daily anomaly of the observed field A associated with the occurrence of an E1_EPE, as in the difference between the mean daily value of A found when the precipitation extreme event is detected in the E1 region, and the corresponding daily climatological value of A:

$$(A_{p99})' = (A_{p99}) - <A> \qquad (1)$$

where (A_{p99}) is the daily mean value of A when an extreme precipitation event is active, and $<A>$ is the daily climatological value of A for the PRESCLI period. The composite anomaly A_{p99} is then calculated as the mean of the daily anomalies $(A_{p99})'$.

In the rest of the paper the term anomaly will refer to anomalies computed as in Equation (1). E1_EPEs associated anomalies are computed for a number of large scale fields up to 7 days prior the extreme event occurrence: "LAG 0" tags the anomaly computed the day in which EPE occurs, "LAG -7" tags the anomaly computed 7 days before. The statistical significance of the anomalies, is verified at the 95% level with a bootstrap method.

3. RESULTS

A measure of the vertically integrated water transport over the North Atlantic basin prior the occurrence of extreme events over the E1 region is shown in Figure 1, where the composite IWT associated with the 32 extreme events is averaged over the 4 days prior and during their occurrence. An evident path appears (IWT zonal and meridional IWT anomaly vector components are shown in Figure 2 and 3), connecting the tropical western North Atlantic to the E1 region. Two main streams seem to be involved in the transport of atmospheric water to the mid-latitudes in the 5 days (4 prior, plus the extreme event day) "corresponding" to E1_EPEs occurrence. The main path is through the western North Atlantic sector, connecting the region east of Florida, north of 30oN, to high latitudes (50oN). A secondary stream involved in poleward water transport is also evident, branching from the central North Atlantic deep tropics at about 50oW in longitude. Both branches start from regions with a very high availability of precipitable water, if compared to the midlatitudes (see blue contour lines in Figure 1). From a climatological point of view, during SON, the PW available south of 30oN is almost doubled when compared to the water availability at E1 region latitudes.

To better understand the time evolution of the atmospheric water transport prior E1_EPEs, in the same composite framework, we computed the IWT anomalies, for each flux component - meridional (Figure 2) and zonal (Figure 3) - highlighting a statistically significant water transport from the tropics to the midlatitudes since 4 days prior the E1_EPEs day. It is important to note that the maxima IWTp99 (Figures 1-3) values found over south western Europe, across Spain and eastern North Atlantic basin at lag 0, are mainly due to the composite cyclonic structure emerging since 4 days prior the E1_EPEs (as represented in Figures 2 and 3) as confirmed by the negative composite surface pressure anomalies (solid blue lines) centred west of the E1 region. This is the Atlantic sector where the cyclonic perturbations develop during the considered season, be-
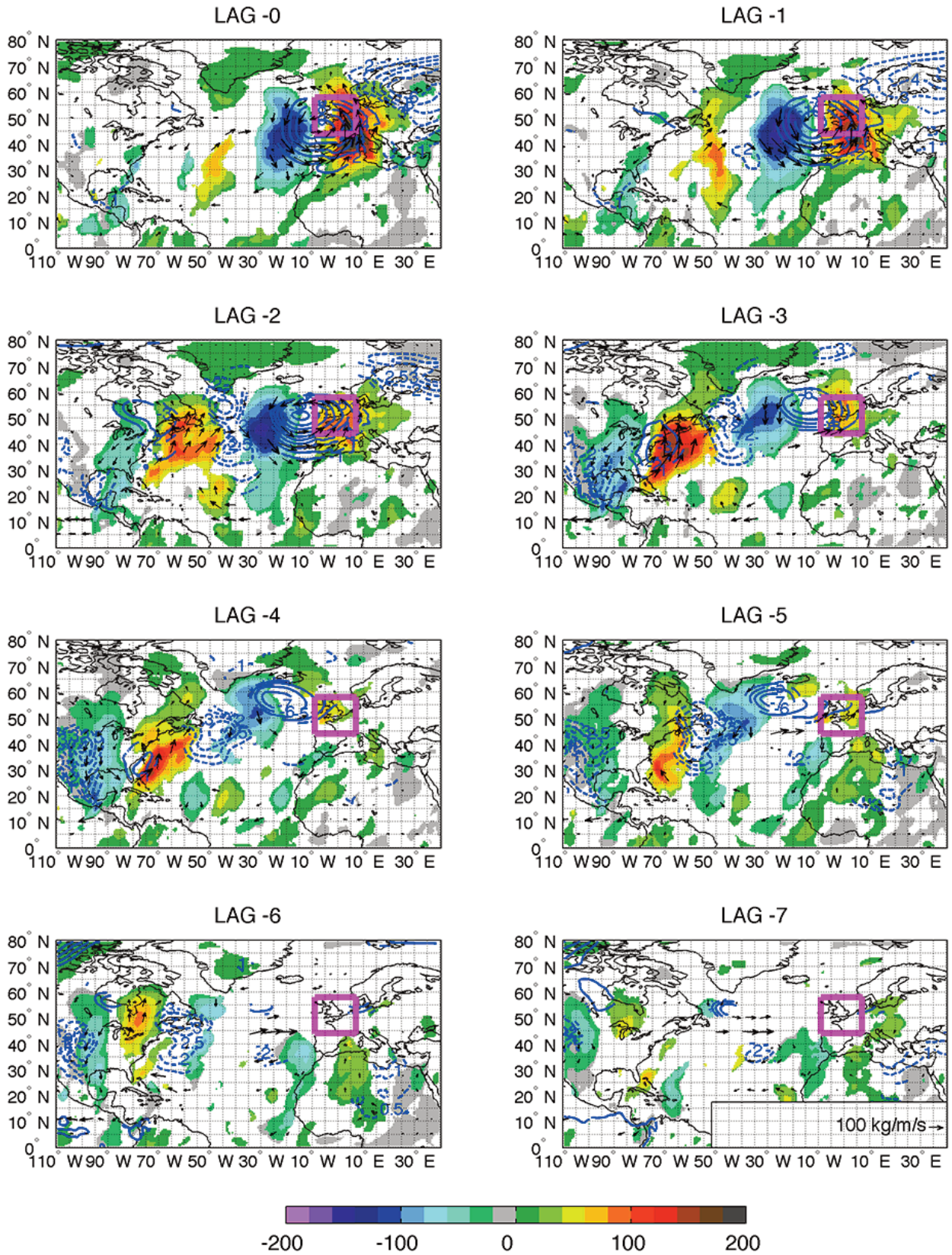
FIGURE 2. Composite of vertically integrated water meridional transport anomalies, VWVp99 (shaded), associated with extreme precipitation events (>99 percentile) over the investigated region (E1, magenta box). Thirty-two events are considered over September-October-November within 1979-2013. Arrows indicate vertically integrated water transport anomalies, IWTp99. Water transport units are [kgm⁻¹s⁻¹]. Dashed/solid blue contours indicates positive/negative surface pressure anomalies, PRESp99. Pressure units are [hPa]. Only significant anomalies are plotted. Lag correlations are back in time and relative to the extreme precipitation day.
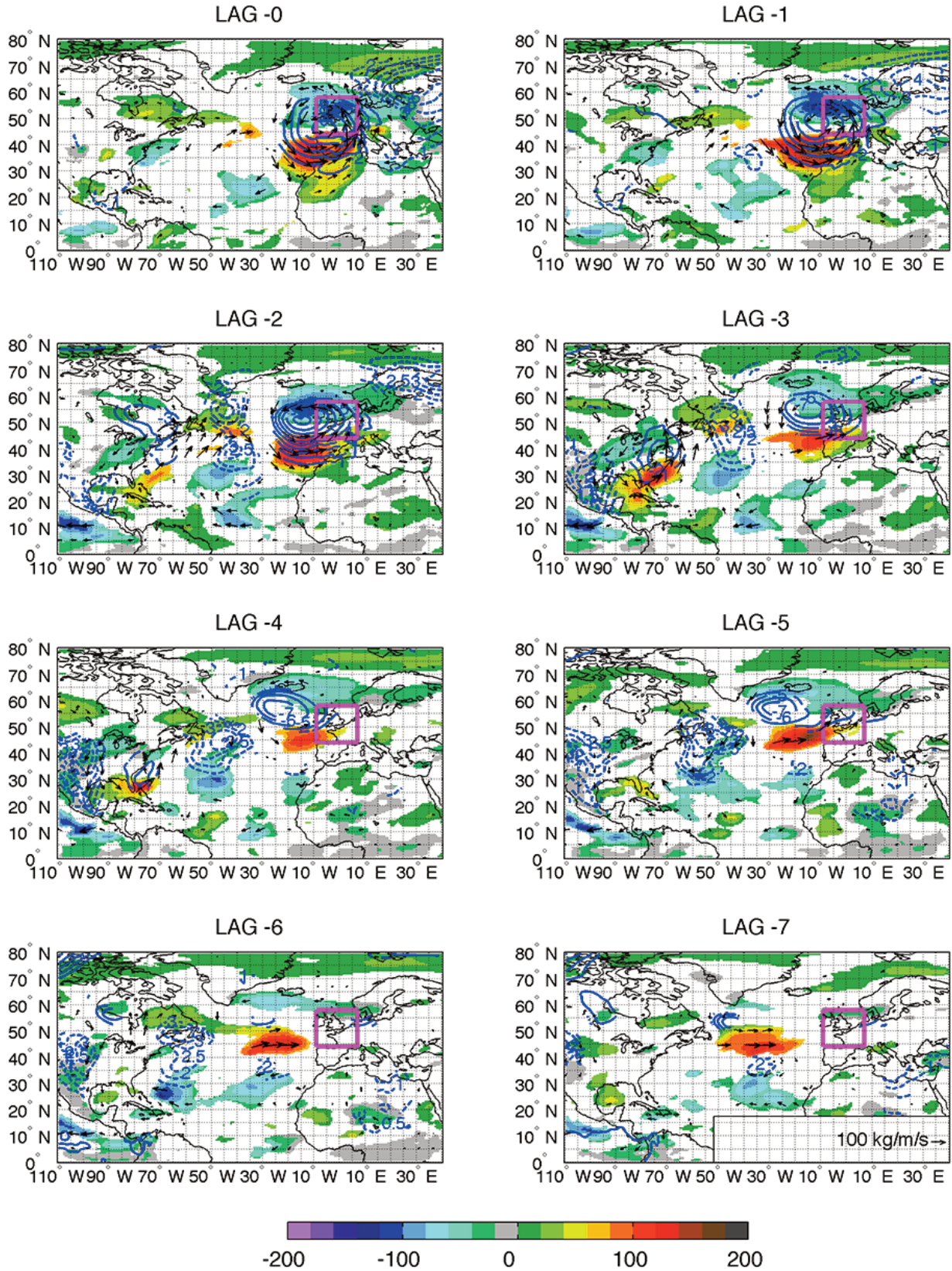
FIGURE 3. Composite of vertically integrated water zonal transport anomalies, UWVp99 (shaded), associated with extreme precipitation events (>99 percentile) over the investigated region (E1, magenta box). Thirty-two events are considered over September-October-November within 1979-2013. Arrows indicate vertically integrated water transport anomalies, IWTp99. Water transport units are [kgm^{-1}s^{-1}]. Dashed/solid blue contours indicates positive/negative surface pressure anomalies, PRESp99. Pressure units are [hPa]. Only significant anomalies are plotted. Lags are back in time and relative to the extreme precipitation day.
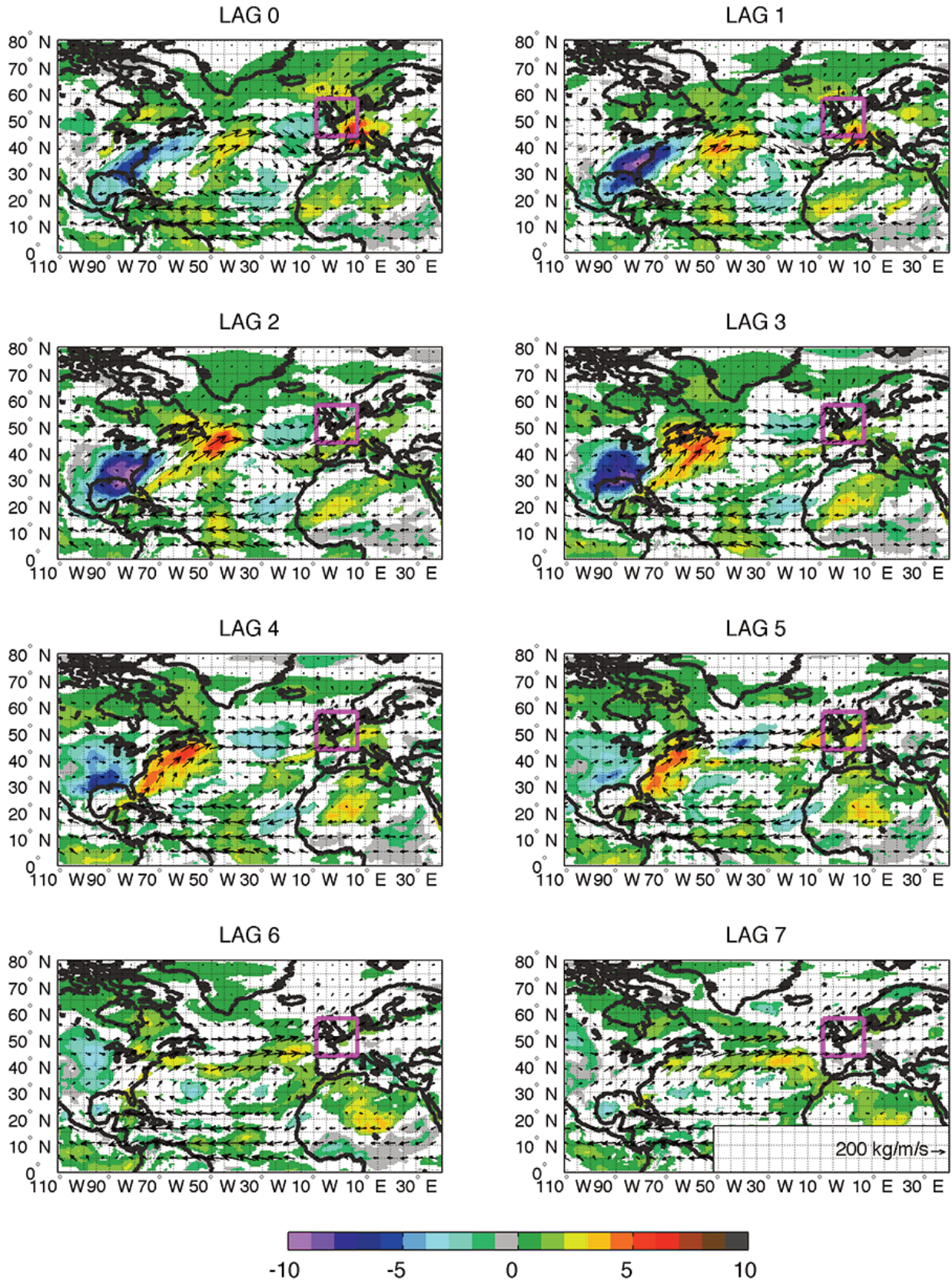
FIGURE 4. Composite of precipitable water anomalies, PWp99 (shaded - only statistically significant anomalies are plotted), associated with extreme precipitation events (>99 percentile) over the investigated region (E1, magenta box). Thirty-two events are considered over September-October-November within 1979-2013. Precipitable water units are [Kgm^{-2}]. Lag correlations are back in time and relative to the extreme precipitation day. Vectors indicate the composite of the vertically integrated water transport [kgm^{-1}s^{-1}].
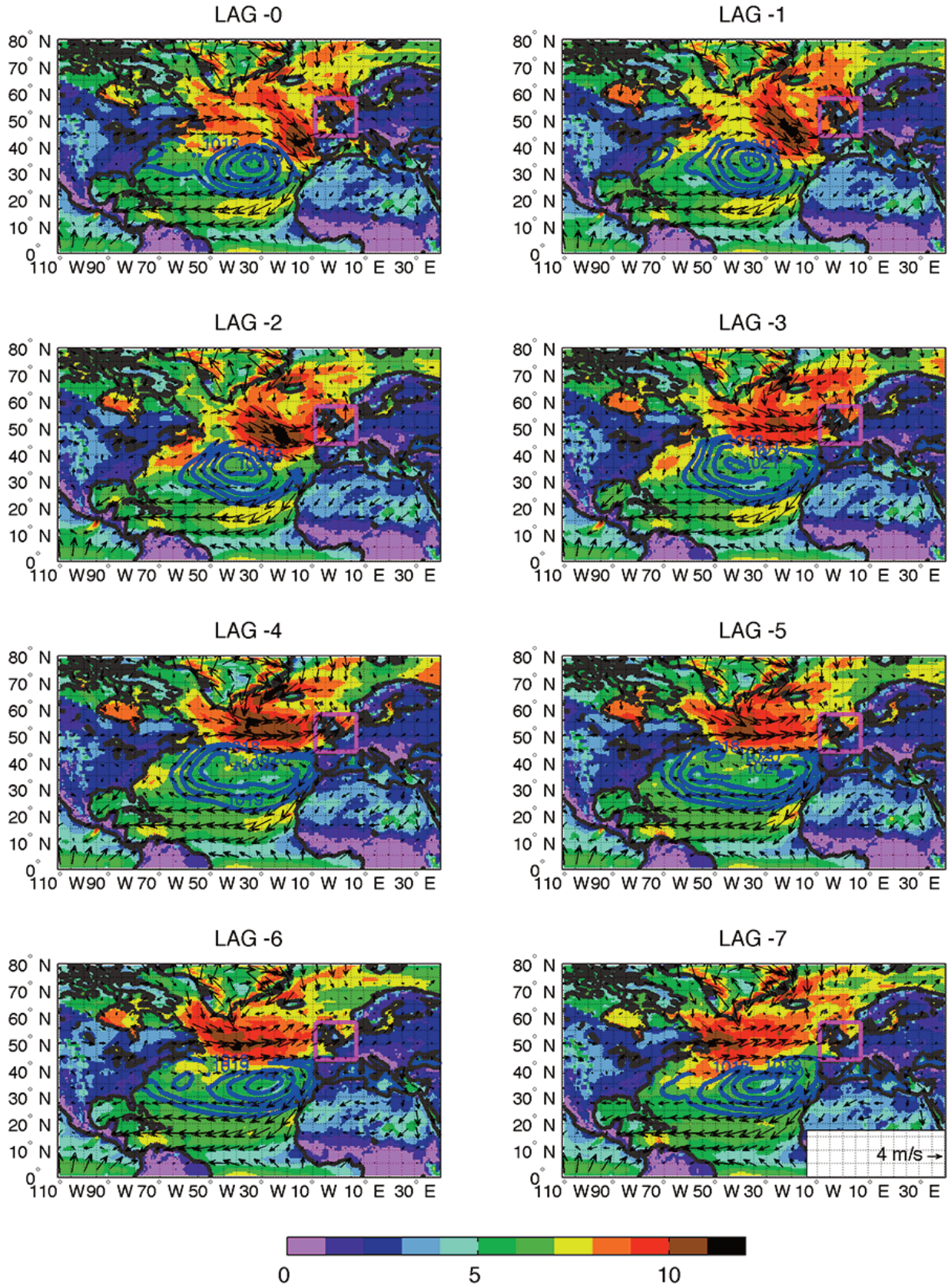
FIGURE 5. Composite of 10 meter wind intensity, (shaded), and direction (arrows) associated with extreme precipitation events (>99 percentile) over the investigated region (E1, magenta box). Thirty-two events are considered over September-October-November within 1979-2013. Wind units are [m/s]. Blue contours indicate composite of surface pressure at the same time. Pressure units are [hPa] and contours between 1018 and 1028 hPa, with a 1 hPa step, are plotted.
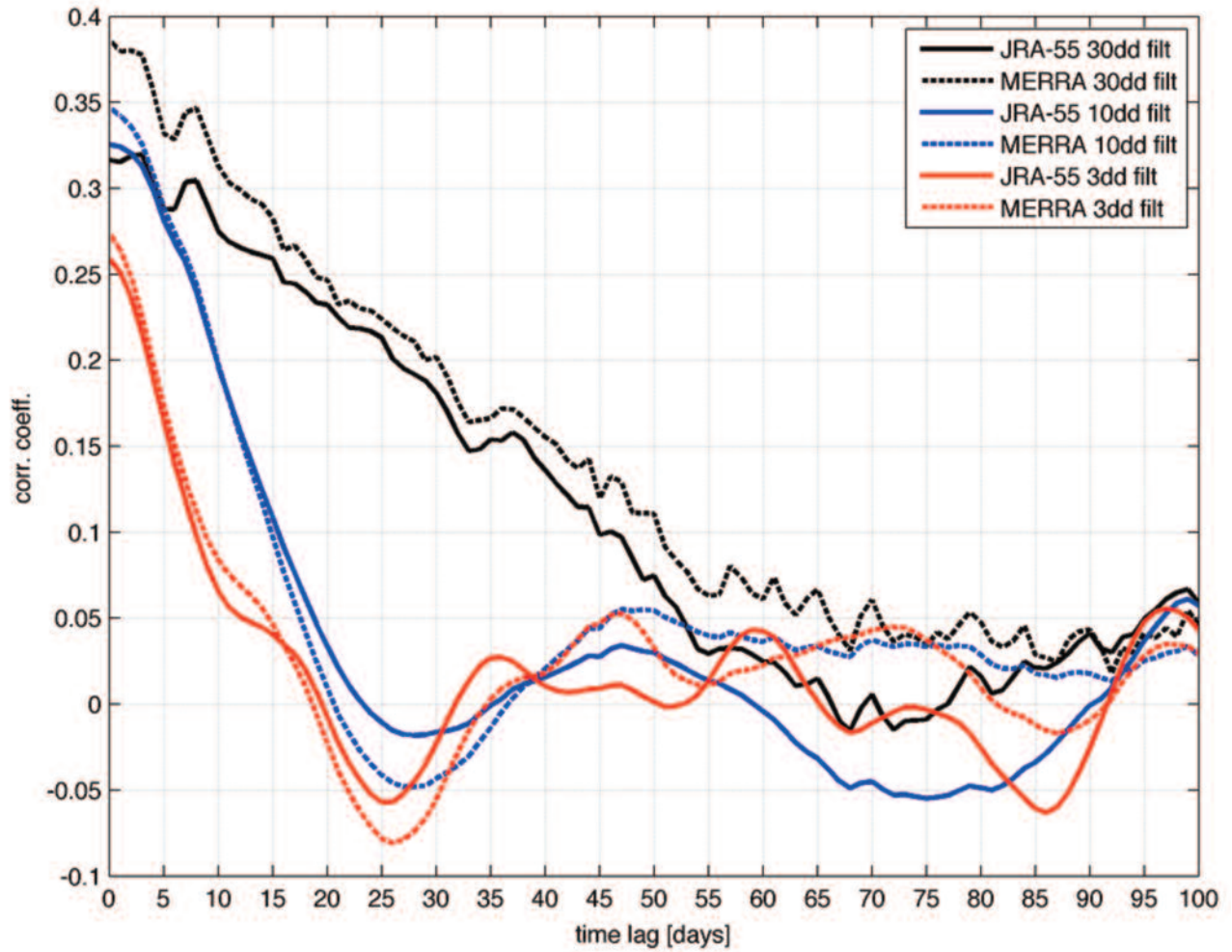
FIGURE 6. Correlation coefficient between surface pressure averaged over the central Atlantic region (40W20W 20N40N) and maximum precipitation over E1 region (magenta box in figure 1) time series, at different time lags (pressure is lagged back in time). Results obtained using different low pass filters on the time series are shown: Black/Blue/Red lines represent results obtained filtering with a 30/10/3 days window. Solid lines represent JRA-55 results. Dashed lines represent MERRA results.

fore hitting the European coast. In fact the vast majority of west-European storms originate from baroclinic instability in the midlatitudes [Haarsma et al., 2013].

Five days prior (LAG -5) the extreme events occurrence in the E1 region, a significant transport of water vapour from the tropics to high latitudes appears in the eastern part of the basin, persisting up to LAG -1, as highlighted by the vertically integrated water transport anomaly components (Figures 2 and 3). Tropical atmospheric water moves poleward and eastward, going from LAG -5 to LAG -1, as shown by the time evolution of precipitable water anomalies (PWp99, Figure 4). At LAG -1 the anomalous amount of water is available to fuel the southern branch of the composite cyclonic perturbation associated with the extreme events over E1 region. The evolution of the positive water transport anomalies originated in the western North Atlantic and

then migrating eastward is evident in Figure 2. At LAG -5, the maximum poleward meridional transport is across the subtropics in the western North Atlantic (red patterns), accompanied by an equatorward transport over North America at approximately the same latitudes (blue patterns). Air masses intruding from high latitudes into the tropics are dryer then the tropical atmosphere, thus a negative IWTp99 is found over the Northern American continent. During the following days (LAG -4 to LAG -2), the water transport anomaly in the western North Atlantic moves eastward (Figure 2) and dominates the patterns until LAG -2, then it decreases. On the other side, over the eastern North Atlantic at higher latitudes, the IWTp99 tends to increase and becomes dominant at LAG -1, in association to the composite cyclonic structure, close to the E1 region. A clearer representation of the water path during the 5

days prior the extreme events over the E1 region is shown in Figure 4 where the absolute value of the composite integrated water transport (arrows) is shown (unlike, arrows in Figure 2 and Figure 3 indicate IWT composite anomalies): the associated water transport from the central western North Atlantic sector to the eastern North Atlantic sector at midlatitudes, follows the IWT climatological path but it is reinforced in magnitude prior extreme events over E1 region, as demonstrated by the statistically significant anomalies found in the vertically integrated water transport. Focusing on the evolution of the surface pressure in the central North Atlantic since one week before the considered extreme events, the surface high pressure pattern (between 20N and 40N) typically extending from U.S. coast to European coast during SON, tends to be less extended since LAG -5, leading to the most pronounced shrinking of the high pressure lobe at LAG -1 (Figure 5). These positive pressure anomalies are coherent with the associated northward/southward increase of IWT in the western/eastern sector (left of the positive pressure lobe) of the central North Atlantic. The highlighted relationship between the high pressure patterns in the central North Atlantic and the extreme precipitation events over the E1 region suggests a potential source of predictability. This is shown in Figure 6 where the correlation coefficients [Spearman, 1904] between the daily time series of the maximum precipitation within the E1 box and the surface pressure averaged over the central North Atlantic (hereafter defined as the box within 40W-20W and 20N-40N) are shown at different time lags. Both JRA-55 and MERRA re-analyses are considered in this Figure. These correlation coefficients tends to decrease when the surface pressure time series is lagged back in time, decreasing to values lower than 0.2 after 4/10/25 days when filtering the time series with a 3/10/30 days time window, trying to reduce the internal variability ('noise'). These findings highlight an increase of the predictive skill when filtering out high frequency variability [Reichler and Roads, 2003]: the signal to noise ratio and thus the potential predictability increase with increased averaging period (see also Figure A6 and A7 in the supplemental material).

4. DISCUSSION AND CONCLUSIONS

A lagged composite analysis of the water transport associated with extreme precipitation events over the E1 region shows that these events are preceded by a pronounced and significant export of water from the western tropical sector of the North Atlantic basin into the mid-latitude central North Atlantic. A reasonable strategy to explain this export may be to link it to the storms developing over these regions and moving northward: the main cyclonic perturbations traveling at these latitudes are Tropical Cyclones (TCs). Indeed, recent studies suggest TCs as a fundamental source of water export from the tropical North Atlantic, feeding extreme events over Europe [Stohl at al., 2008; Krichak et al., 2015]. Despite these findings, in the present study just few [8 over 32) extreme events happens after TCs passage in the North Atlantic. Besides, 5 of these 8 appear to develop in the central North Atlantic [cluster 2 type TCs, as from Daloz et al., 2014], thus they do not affect the eastern coast of U.S., where the northward export of atmospheric water vapour appears to occur since 4 days prior the considered extreme events. These five TCs are the main responsible for the water transport branch shown in Figure 1 at around 50oW longitude. On the other hand, two of the 8 TCs occurring prior extreme events over the E1 region (not shown) developed over the western North Atlantic. Therefore, from this study there are no evidences that TCs are the main responsible for the export of water vapour from western Tropical Atlantic, fuelling E1_EPEs, but we would link it to any kind of atmospheric condition leading to a reinforced - significantly higher than the climatology - poleward export of atmospheric water from the "tropical source". We also found statistically significant anomalous circulation patterns over the North Atlantic basin associated with extreme precipitation events over the Europe's Atlantic coast, forming 5 days prior their occurrence. The composite anomalous anti-cyclonic structure appearing over the central North Atlantic (Figure 5) 5 days before the E1_EPEs occurrence (see also Figure 2 and Figure 3) contributes to reinforcing the net export of atmospheric water to high latitudes, fuelling the storms bound to affect the E1 region at LAG 0. This specific mechanism requires a deeper analysis in a future work.

It is well known that extreme hydrological events over Europe are connected with intense water vapour transport and this study provides further evidence that the North Atlantic sector acts as a source of moist air for extreme precipitation events over Europe [Pinto et al., 2009; Pinto et al., 2013; Lavers et al., 2013; Krichak et al., 2015]. For this reason, Lavers et al. [2014] leveraged on the transport predictability to extend the extreme events forecast horizon by 3 days in some European regions. We found that the spatial extension and the intensity of surface pressure maxima in the central North Atlantic might be a viable tool to predict anomalous northward IWT, and thus of extreme precipitation oc-

currence over the considered regions, with a correlation greater than 0.3 between surface pressure averaged over the central Atlantic region and maximum precipitation over the E1, up to 5 days prior the event (Figures 6 and S6). Noteworthy, associated with the described anomalous anti-cyclonic structure, on its western side, there is a consistent and significant increase in the surface evaporation fluxes over the Gulf of Mexico and off Florida coasts since 4 days prior (LAG -4) extreme events over E1 region (not shown). Further studies are needed to verify the predictive skill of both surface pressure in the central North Atlantic and evaporation fluxes in the western Atlantic in forecasting extreme precipitation events over the Europe's Atlantic coast.

Despite a slightly different timing of the extreme events occurrence in the considered 35 years period over the investigated region, very similar results emerge using MERRA instead of JRA-55 re-analyses (Figure 6 and Figures S1-S5, S7 in the supplemental material), strengthening our conclusions.

REFERENCES

Dacre, H.F., P.A. Clark, O. Martinez-Alvarado,M.A. Stringer, and D.A. Lavers (2015). How do atmospheric rivers form?, Bulletin of the American Meteorological Society. http://dx.doi.org/10.1175/BAMS-D-14-00031.1

Daloz A.S., et al. (2014). Cluster analysis of explicitly and downscaled simulated North Atlantic tropical cyclone tracks J. of climate, doi: 10.1175/JCLI-D-13-00646.1.

Dettinger, M., Ralph, F. M., and Lavers, D. (2015). Setting the stage for a global science of atmospheric rivers, Eos, 96, doi:10.1029/2015EO038675.

Gimeno L., A. Drumond, R. Nieto, R. M. Trigo, and A. Stohl (2010a). On the origin of continental precipitation, Geophys. Res. Lett, 37, L13804, doi:10.1029/2010GL043712.

Gimeno L., Nieto R., Trigo R.M., Vicente-Serrano S.M., Lopez-Moreno J.l. (2010b). Where does the Iberian Peninsula moisture come from? An answer based on a Lagrangian approach. J Hydrometeorol;11(2):421-436.

Haarsma, R.J., W. Hazeleger, C. Severijns, H. de Vries, A. Sterl, R. Bintanja, G.J. van Oldenborgh and H.W. van den Brink (2013). More hurricanes to hit Western Eu-

rope due to global warming. Geophys. Res. Lett., 2013, doi:10.1002/grl.50360.

Knippertz P., and H. Wernli (2010). A Lagrangian Climatology of Tropical Moisture Exports to the Northern Hemispheric Extratropics J. of Climate. 23, 987-1003. doi: http://dx.doi.org/10.1175/2009JCLI3333.1.

Kobayashi, S., Y. Ota, Y. Harada, A. Ebita, M. Moriya, H. Onoda, K. Onogi, H. Kamahori, C. Kobayashi, H. Endo, K. Miyaoka, and K. Takahashi (2015). The JRA-55 Reanalyses: General Specifications and Basic Characteristics. J. Meteor. Soc. Japan, 93, doi: 10.2151/jmsj.2015-001.

Krichak, S.O., J.S. Breitgand, and S.B. Feldstein, (2012). A conceptual model for the identification of active Red Sea Trough synoptic events over the southeastern Mediterranean. J. Appl. Meteor. Climatol., 51, 962-971. D\doi: http://dx.doi.org/10.1175/JAMC-D-11-0223.1.

Krichak S.O., Barkan J., Breitgand J.S., Gualdi S., and Feldstein S.B., (2015). The role of the export of tropical moisture into midlatitudes for extreme precipitation events in the Mediterranean region Theor Appl Climatol doi:10.1007/s00704-014-1244-6.

Kudo, T., R. Kawamura, H. Hirata, K. Ichiyanagi,M. Tanoue, and K. Yoshimura, (2014). Large-scale vapor transport of remotely evaporated seawater by a Rossby wave response to typhoon forcing during the Baiu/Meiyu season as revealed by the JRA-55 re-analyses, J. Geophys. Res. Atmos., 119, 8825-8838, doi:10.1002/2014JD021999.

Lavers, D. A., R. P. Allan, E. F. Wood, G. Villarini, D. J. Brayshaw, and A. J. Wade, (2011). Winter floods in Britain are connected to atmospheric rivers, Geophys. Res. Lett., 38, L23803, doi:10.1029/2011GL049783.

Lavers, D.A., and G. Villarini, (2013). The nexus between atmospheric rivers and extreme precipitation across Europe. Geophys. Res. Lett., 40, 3259-3264.

Lavers, D.A., Pappenberger F, and Zsoter E., (2014). Extending medium-range predictability of extreme hydrological events in Europe. Nature Communications. 5:5382.

Lavers D.A., R.P. Allan, G. Villarini , B. Lloyd-Hughes , D.J. Brayshaw and A.J. Wade, (2013). Future changes in atmospheric rivers and their implications for winter flooding in Britain. Env. Res. Lett. 8, 034010 (8pp).

Nayak, M.A., and G. Villarini, (2017). A long-term perspective of the hydroclimatological impacts of atmospheric rivers over the central United States, Water Resources Research, 53, 1144-1166.

Newell, R. E., N. E. Newell, Y. Zhu, and C. Scott (1992). Tropospheric rivers? A pilot study. Geophys. Res. Lett., 19, 2401-2404.

Pauluis, O., A. Czaja, and R. Korty (2008). The global atmospheric circulation on moist isentropes. Science, 321, 1075-1078.

Pinto J.G. Zacharias S., Fink A.H. Leckebusch G.C., and Ulbrich U. (2009). Factors contributing to the development of extreme North Atlantic cyclones and their relationship with the NAO, Clim. Dyn. 32:711-737, doi: 10.1007/s00382-008-0396-4.

Pinto J.G., S. Ulbrich, A. Parodi, R. Rudari, G. Boni, and U. Ulbrich (2013). Identification and ranking of extraordinary rainfall events over Northwest Italy: The role of Atlantic moisture, J. Geoph. Res. Atm., 118, 2085-2097, doi:10.1002/jgrd.50179.

Ralph F.M., and Dettinger M.D. (2011). Storms, floods, and the science of atmospheric rivers, EOS, Transactions, American Geophysical Union, 92, 32, 265-272.

Ramos, A. M., Nieto, R., Tomé, R., Gimeno, L., Trigo, R. M., Liberato, M. L. R., and Lavers, D. A. (2016). Atmospheric rivers moisture sources from a Lagrangian perspective, Earth Syst. Dynam., 7, 371-384, doi:10.5194/esd-7-371-2016.

Reichler, T. and J. O. Roads, (2003). The role of boundary and initial conditions for dynamical seasonal predictability. Nonlinear Proc Geophys. 10: 211-232.

Rienecker, M., et al. (2011). MERRA: NASA's Modern-Era Retrospective Analysis for Research and Applications, J. Clim., 24, 3624-3648, doi: 10.1175/JCLI-D-11-00015.1.

Spearman C. (1904). The proof and measurement of association between two things. American Journal of Psychology 15: 72-101.

Stohl, C. F. and H. Sodemann (2008). Remote sources of water vapor forming precipitation on the Norwegian west coast at 60_N-a tale of hurricanes and an atmospheric river, J. Geophys. Res. 113, D05102, doi:10.1029/2007JD009006.

Talagrand, O., and P. Courtier (1987). Variational assimilation of meteorological observations with the adjoint vorticity equation. I-Theory. Quart. J. Roy. Meteor. Soc., 113, 1311-1328.

Walker, C. C., and T. Schneider (2006). Eddy influences on Hadley circulations: Simulations with an idealized GCM. J. Atmos. Sci., 63, 3333-3350.

Winschall A, H. Sodemann, S. Pfahl, H. Wernli. (2014). How important is intensified evaporation for Mediterranean precipitation extremes? J. Geophys. Res. 119, 9, 5240-5256. doi: 10.1002/2013JD021175.

*CORRESPONDING AUTHOR: Enrico SCOCCIMARRO,

Fondazione CMCC,

Bologna, Italy

email: enrico.scoccimarro@cmcc.it

EXTREME PRECIPITATION EVENTS OVER NORTH-WESTERN EUROPE: GETTING WATER FROM THE TROPICS

Enrico Scoccimarro[1], Silvio Gualdi[1,2], Simon O. Krichak[3]

[1]Fondazione Centro Euro-Mediterraneo sui Cambiamenti Climatici (CMCC), Bologna, Italy
[2]Istituto Nazionale di Geofisica e Vulcanologia (INGV), Bologna, Italy
[3]Department of Geosciences, Raymond and Beverly Sackler Faculty of Exact Sciences, Tel Aviv University, Tel Aviv, Israel
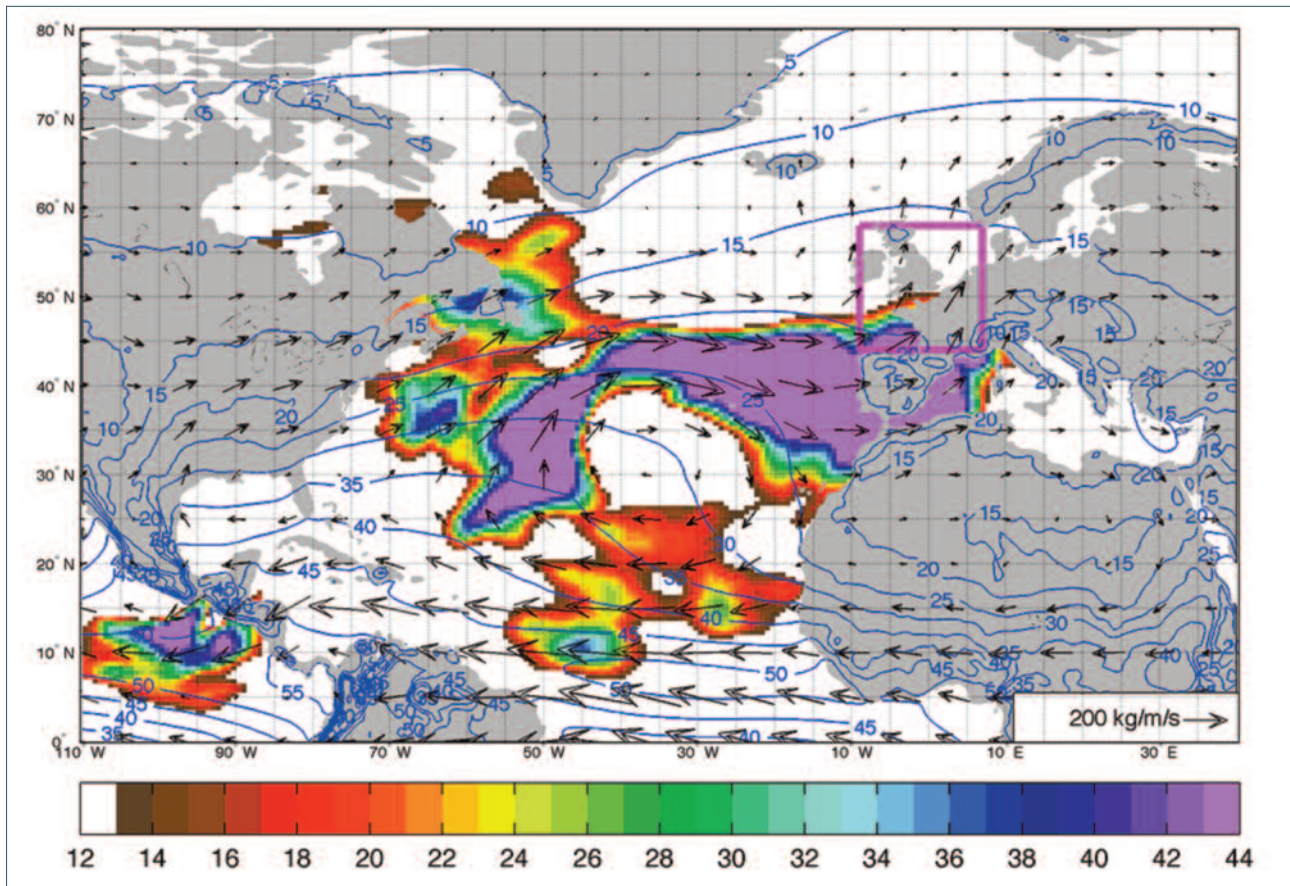
FIGURE S1. Same as Figure 1, but based on MERRA reanalyisis instead of JRA-55. Composite of vertically integrated water transport IWT associated to E1_EWEs, averaged over the four days prior the extreme precipitation events and E1_EWEs day. Color patterns are IWT absolute value composite anomalies (IWTp99). Vectors are IWT composites over the E1_EWEs, averaged over the same period, same as IWTp99, but these are not anomalies. Contour lines represent precipitable water SON (PW) climatology. IWT Units are $[kgm^{-1}s^{-1}]$. PW Units are $[Kgm^{-2}]$.
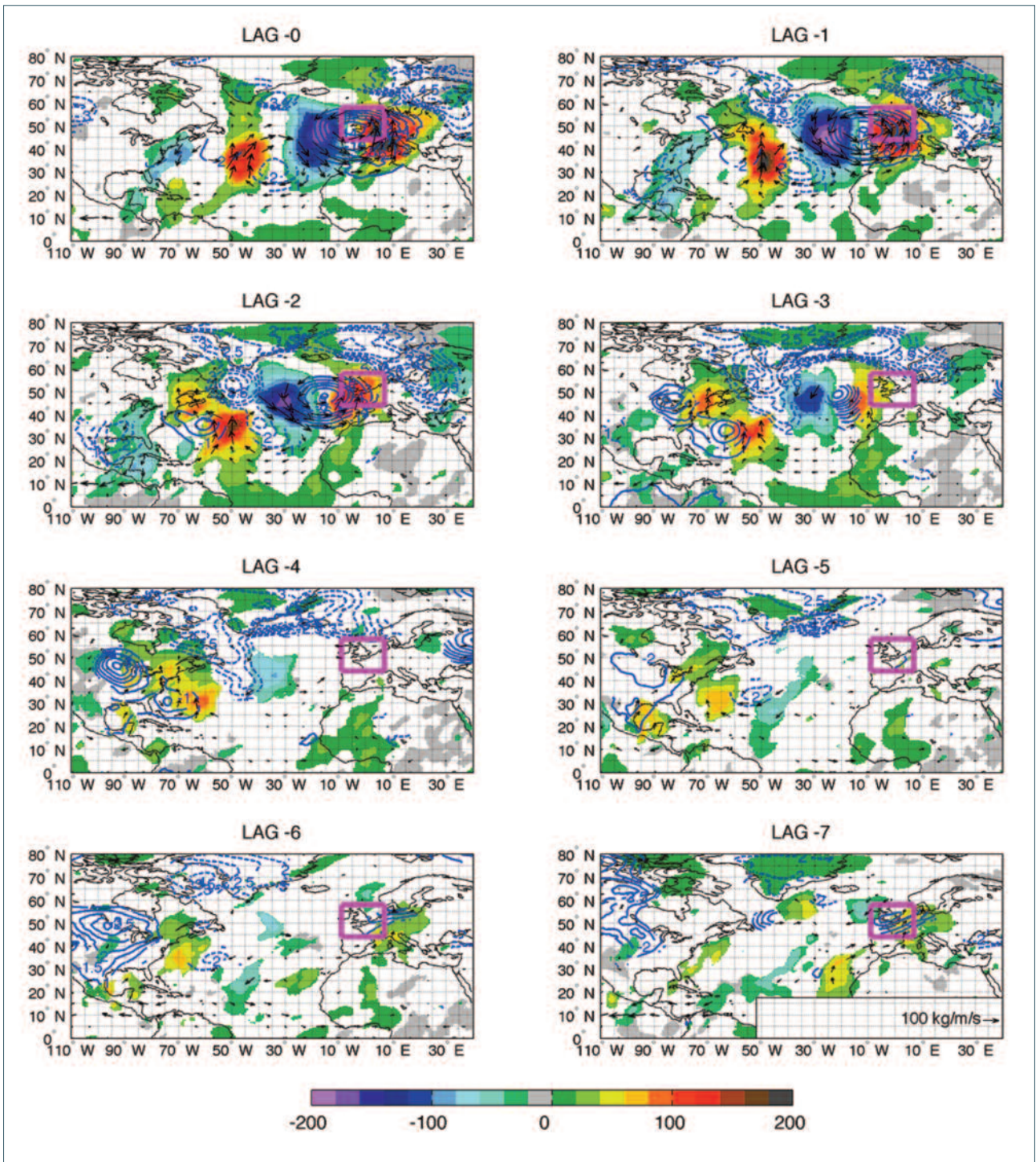
FIGURE S2. Same as Figure 2, but based on MERRA reanalyisis instead of JRA-55.Composite of vertically integrated water meridional transport anomalies, VWVp99 (shaded), associated to extreme precipitation events (>99 percentile) over the investigated region (E1, magenta box). Thirty-two events are considered over September-October-November within 1979-2013. Arrows indicate vertically integrated water transport anomalies, IWTp99. Water transport units are [kgm-1s^{-1}]. Dashed/solid blue contours indicates positive/negative surface pressure anomalies, PRESp99. Pressure units are [hPa]. Only significant anomalies are plotted. Lag correlations are back in time and relative to the extreme precipitation day.
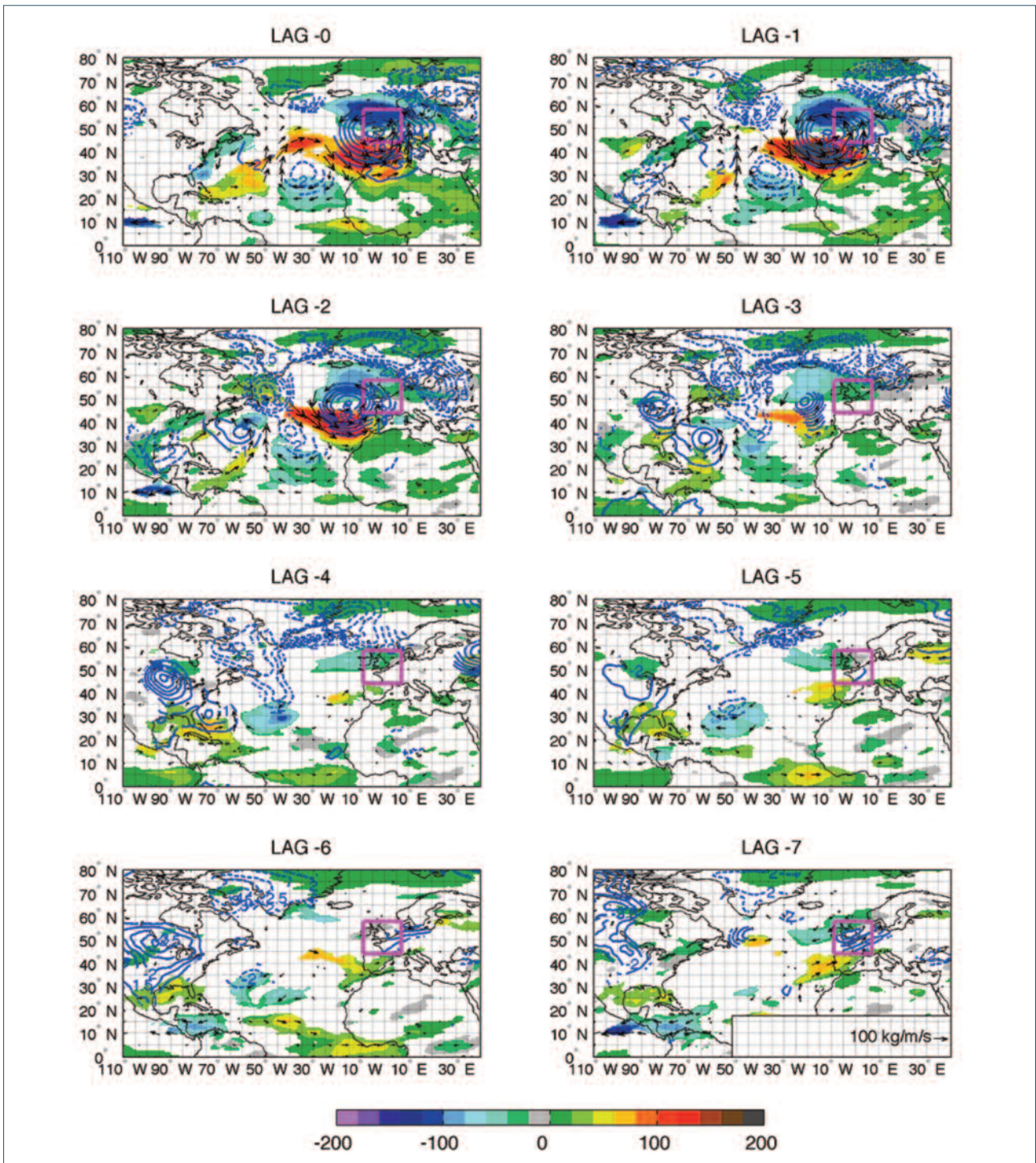
FIGURE S3. Same as Figure 3, but based on MERRA reanalyisis instead of JRA-55. Composite of vertically integrated water zonal transport anomalies, UWVp99 (shaded), associated to extreme precipitation events (>99 percentile) over the investigated region (E1, magenta box). Thirty-two events are considered over September-October-November within 1979-2013. Arrows indicate vertically integrated water transport anomalies, IWTp99. Water transport units are [kgm^{-1}s^{-1}]. Dashed/solid blue contours indicates positive/negative surface pressure anomalies, PRESp99. Pressure units are [hPa]. Only significant anomalies are plotted. Lags are back in time and relative to the extreme precipitation day.
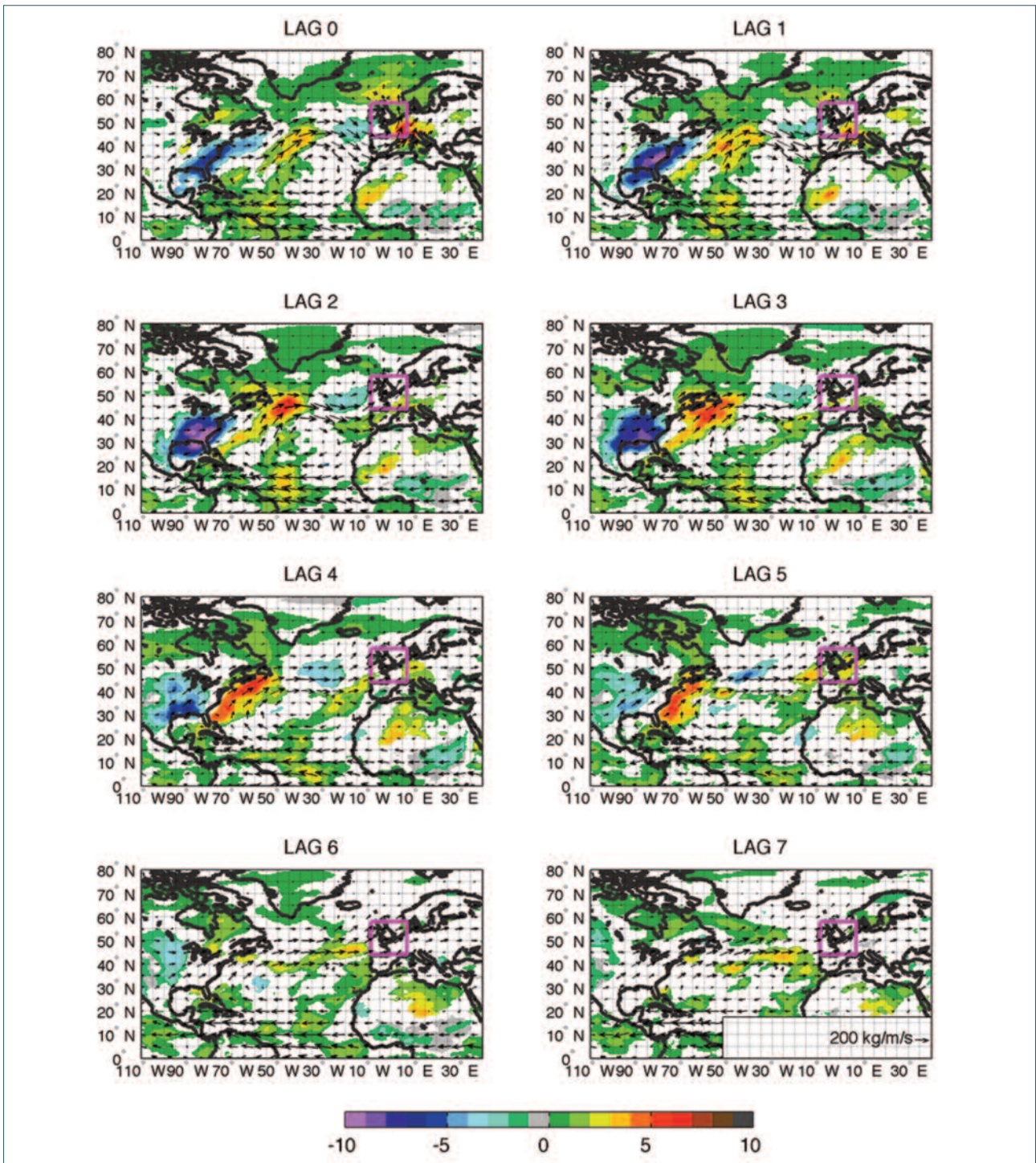
FIGURE S4. Same as Figure 4, but based on MERRA reanalyisis instead of JRA-55. Composite of precipitable water anomalies, PWp99 (shaded – only statistically significant anomalies are plotted), associated to extreme precipitation events (>99 percentile) over the investigated region (E1, magenta box). Thirty-two events are considered over September-October-November within 1979-2013. Precipitable water units are [Kgm^{-2}]. Lag correlations are back in time and relative to the extreme precipitation day. Vectors indicate the composite of the vertically integrated water transport [$kgm^{-1}s^{-1}$].
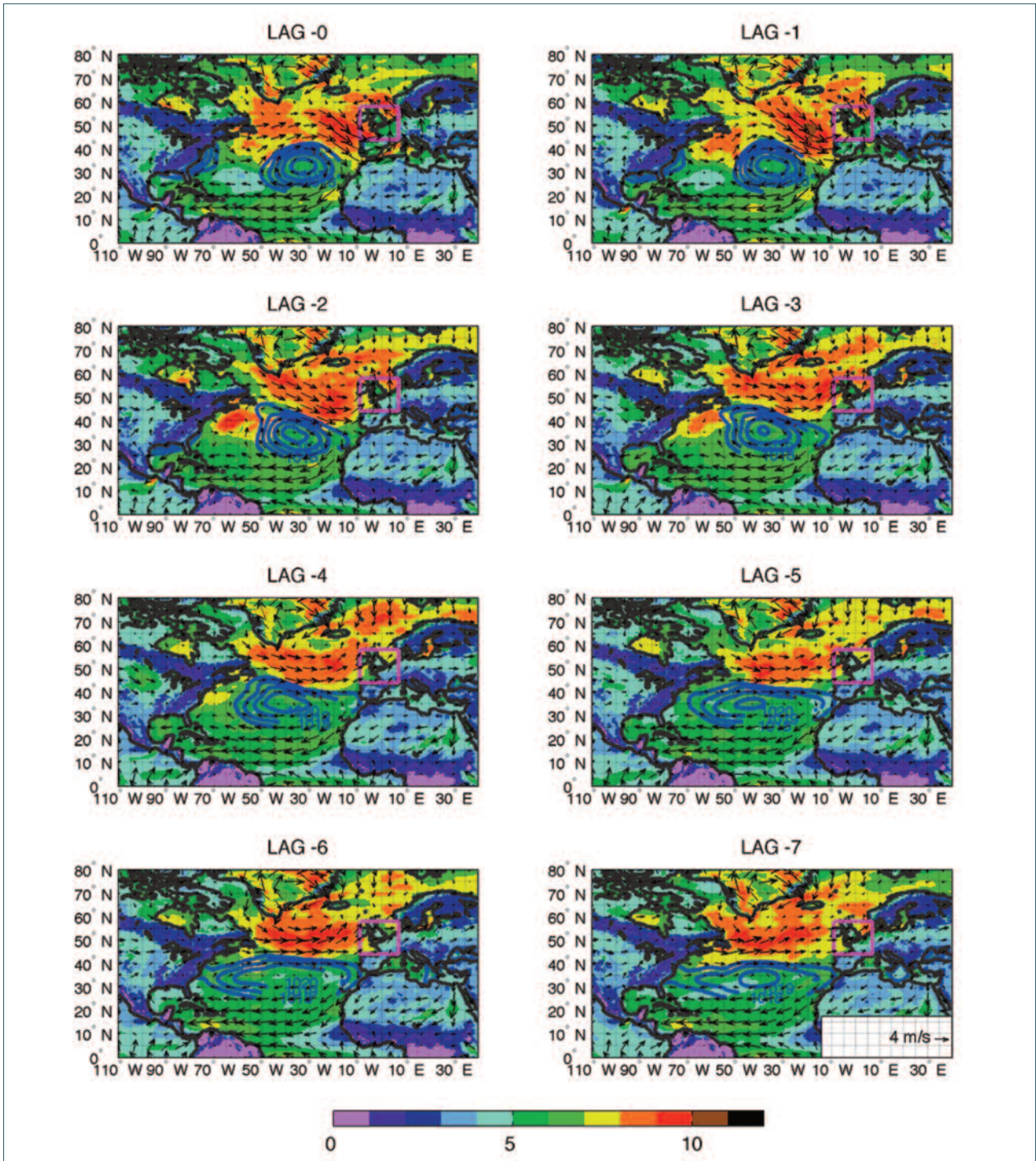
FIGURE S5. Same as Figure 5, but based on MERRA reanalyisis instead of JRA-55. Composite of 10 meter wind intensity, (shaded), and direction (arrows) associated to extreme precipitation events (>99 percentile) over the investigated region (E1, magenta box). Thirty-two events are considered over September-October-November within 1979-2013. Wind units are [m/s]. Blue contours indicates composite of surface pressure at the same time. Pressure units are [hPa] and countours between 1018 and 1028 hPa, with a 1 hPa step, are plotted.
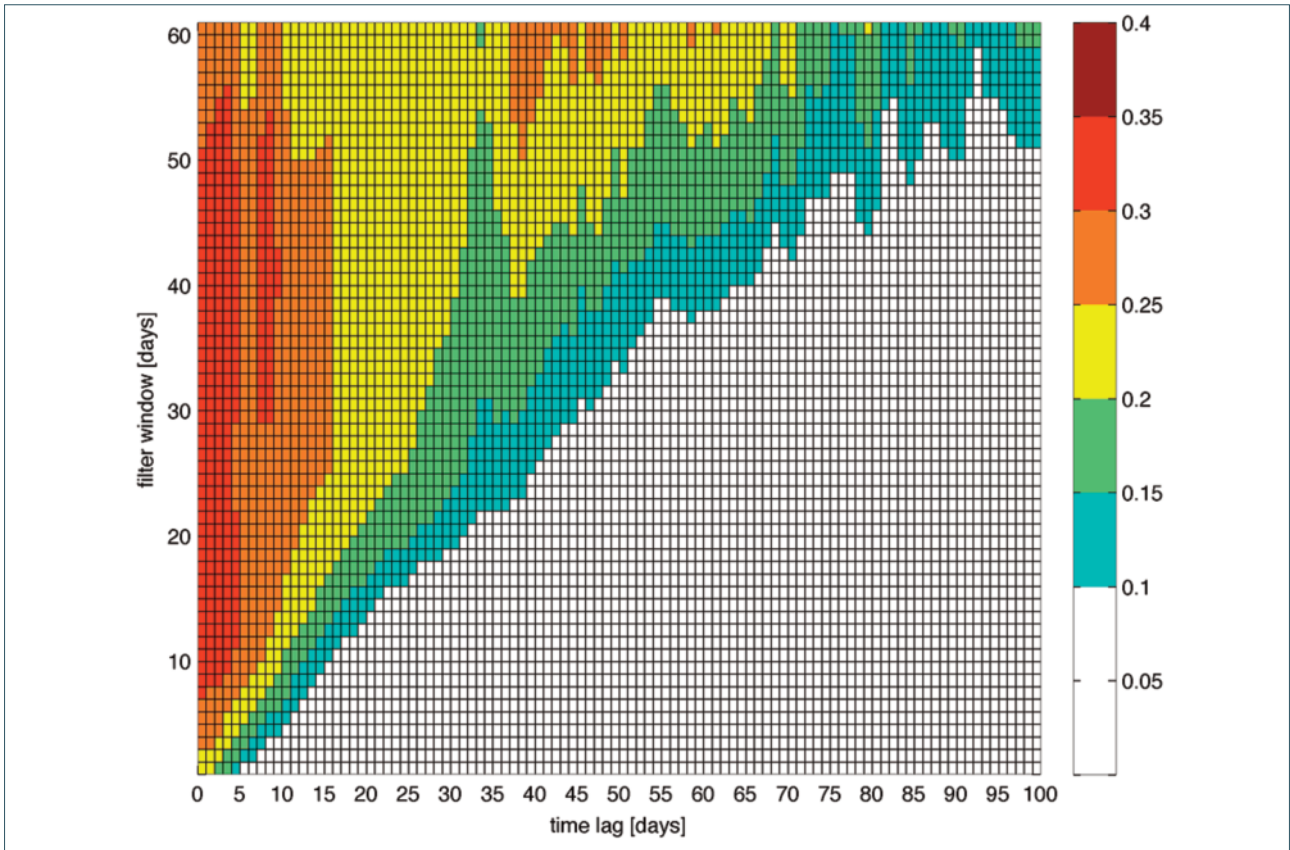
FIGURE S6. Extended representation of Figure 6 based on JRA-55 reanalysis only. Correlation coefficient between surface pressure averaged over the central Atlantic region (40W20W 20N40N) and maximum precipitation over E1 region (magenta box in Figure 1) time series, at different time lags (pressure is lagged back in time). Results obtained using different low pass filters, from 0 to 60 days (y axis) are shown based on different time lags (x axis).
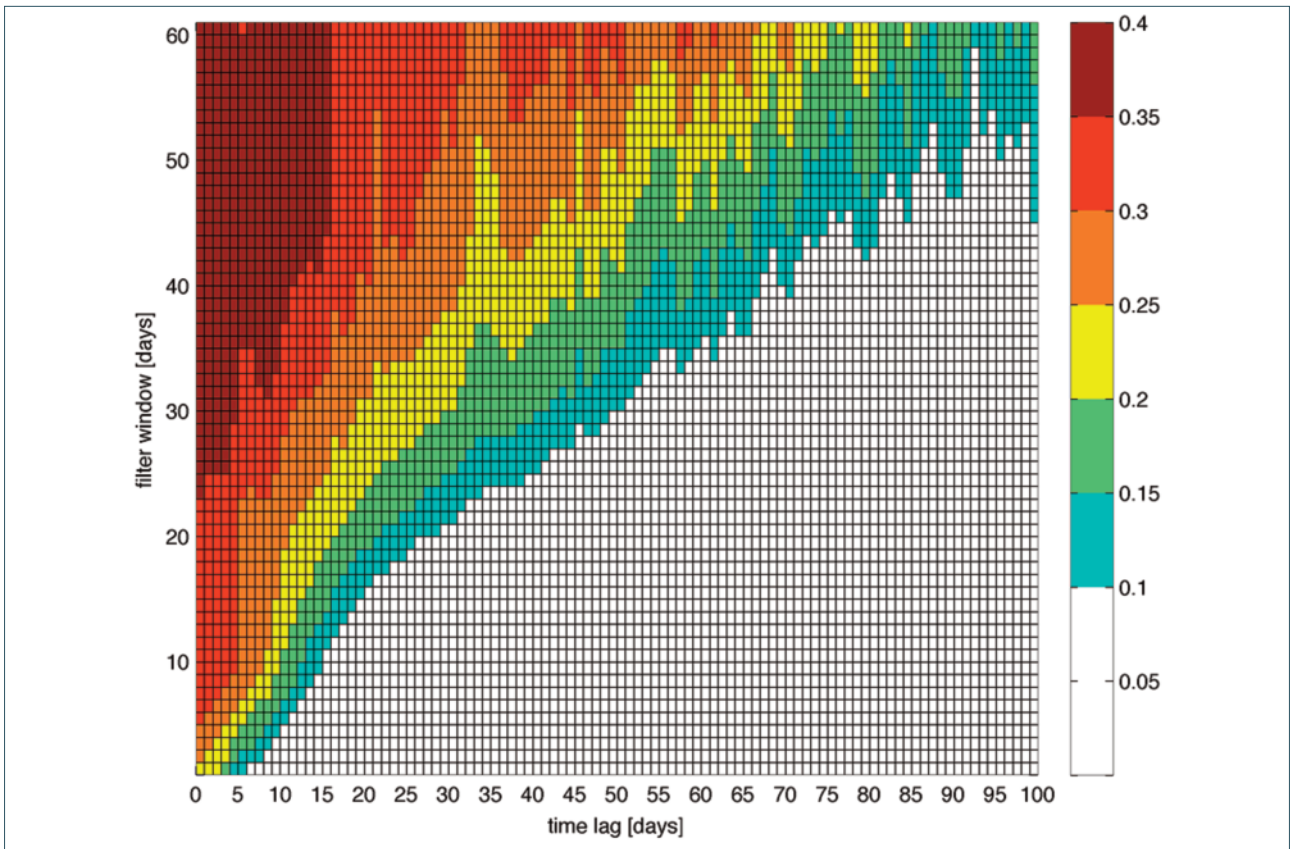

FIGURE S7. Extended representation of Figure 6 in the manuscript based on MERRA reanalysis only. Correlation coefficient between surface pressure averaged over the central Atlantic region (40W20W 20N40N) and maximum precipitation over E1 region (magenta box in Figure 1) time series, at different time lags (pressure is lagged back in time). Results obtained using different low pass filters, from 0 to 60 days (y axis) are shown based on different time lags (x axis).